Villa et al. Annals of Microbiology (2021) 71:3
https://doi.org/10.1186/s13213-020-01617-1

Annals of Microbiology

UNIVERSITÀ DEGLI STUDI DI MILANO

SHORT COMMUNICATION Open Access

Biochemical and molecular changes of the zosteric acid-treated *Escherichia coli* biofilm on a mineral surface

Federica Villa[1*], Francesco Secundo[2], Fabio Forlani[1], Cristina Cattò[1] and Francesca Cappitelli[1]

Abstract

Purpose: The main goal of the present work was to assess the effectiveness of zosteric acid (ZA) in hindering *Escherichia coli* biofilm formation on a mineral surface.

Methods: Attenuated total reflectance-Fourier transform infrared (ATR-FTIR) flow system was used to probe in situ the biochemical changes induced by ZA on *E. coli* sessile cells growing on the zinc selenide ATR plate. Comparative proteome analysis was conducted on the sessile cells to better understand the principal molecular changes that occur on ZA-treated biofilms.

Results: The ZA treatment modified the kinetics of the biofilm development. After the ZA exposure, dramatic changes in the carbohydrates, proteins, and DNA profiles were observed over time in the ATR-FTIR spectra. These results were translated into the physiological effects such as the reduction of both the biomass and the EPS contents, the inhibition of the biofilm growth, and the promotion of the detachment. In *E. coli* sessile cells, the comparative proteome analysis revealed that, while the stress responses were upregulated, the pathways belonging to the DNA replication and repair were downregulated in the ZA-treated biofilms.

Conclusions: The ZA reduced the binding capability of *E. coli* cells onto the ZnSe crystal, hindering the firm adhesion and the subsequent biofilm development on a mineral surface. The variation of the protein patterns indicated that the ZA acted as a stress factor on the sessile cells that seemed to discourage biomass proliferation, consequently decreasing the surface colonization.

Keywords: Zosteric acid, *Escherichia coli* biofilm, Ceramic surface, ATR-FTIR, Proteomic

Findings

The world is united on the view that no surface escapes bacterial colonization, including mineral surfaces. Mineral surfaces are widely used in chemical, engineered, and artistic systems, where biofilms—complex communities encased in a matrix—pose a severe threat to the structures and to human and environmental health despite the availability of control measures (Galié et al. 2018; Li et al. 2018; Chan et al. 2019; Procópio 2019). Because of the health and environmental concerns, together with the increasingly restrictive regulations aimed at limiting the use of dangerous substances, the continuing extensive use of biocide is intensely debated, discouraging the use of such compounds. Thus, new alternatives to replace or to integrate the presently dominating biocide regime are urgently required.

As the surface-bacteria interaction is one of the most important nodes in the bacterial colonization network, the ability to hinder the microbial adhesion and the subsequent biofilm formation may offer a promising opportunity for the development of a new weapon against unwanted biofilms. This action would not necessarily kill the cell, but rather prevent or attenuate the surface colonization by denying access to the substratum

* Correspondence: federica.villa@unimi.it
[1]Dipartimento di Scienze per gli Alimenti, la Nutrizione e l'Ambiente, Universita` degli Studi di Milano, via Celoria 2, 20133 Milan, Italy
Full list of author information is available at the end of the article

through maintenance of the planktonic phenotype. Interfering with the surface sensing process without affecting bacteria viability may also sidestep drug resistance extending the effectiveness of the current arsenal of antimicrobial agents. In this context, the use of bio-inspired molecules to interfere with the formation of deleterious biofilms in sublethal doses represents an ideal strategy worth pursuing. The new strategy consists of interfering with the key-steps that orchestrate biofilm genesis; thus, the colonization cascade might be hampered (Cattò et al. 2018a, 2018b).

In the light of these considerations, zosteric acid (ZA) becomes a powerful antibiofilm agent that can significantly reduce both bacterial and fungal adhesion to polymeric surfaces at sub-lethal concentrations and can successfully counteract the effects of colonization-promoting factors such as temperature, time, and pH (Villa et al. 2010; Villa et al. 2011).

ZA mechanism of action against *Escherichia coli* planktonic cells was elucidated. The comparative proteomic study on *E. coli* planktonic cells exposed to ZA showed that ZA acts as an environmental cue that leads to global stress on the bacterial cells. This induced stress promotes the expression of various stress-response proteins, the signal molecule autoinducer-2, and the synthesis of flagella, to escape from adverse conditions (Villa et al. 2012). The protein WrbA (NADH:quinone reductase) is the molecular target of ZA, suggesting the possible role of this protein in the biofilm formation process and in the ZA antibiofilm activity (Cattò et al. 2015).

Despite such promising results, the antibiofilm performances of ZA on mineral surfaces have not been investigated yet, as well as its mechanisms of action against the sessile cells.

In light of the above considerations, the main goal of the present work was to investigate the effectiveness of ZA in hindering *E. coli* biofilm formation on mineral surfaces. To this end, attenuated total reflectance-Fourier transform infrared (ATR-FTIR) flow system was used to probe in situ the biochemical changes induced by the antibiofilm compound on *E. coli* sessile cells growing on the zinc selenide (ZnSe) crystal of the ATR cell. A better understanding of ZA antibiofilm action is possible only by delving into its molecular mechanisms of action against sessile bacteria inside the biofilms. Thus, the analyses were extended to the proteomic level to better understand the principal molecular changes that occur on the treated biofilms.

The best characterized *E. coli* strain K-12 (American Type Culture Collection ATCC 25404, wild-type) was used throughout the study. *E. coli* is a well-studied biofilm model system, as it is able to colonize a variety of surfaces including stainless steel, PTFE (Teflon), glass, polystyrene, polypropylene, PVC, and biotic surfaces (Beloin et al. 2008; Galié et al. 2018). The microorganism was maintained at − 80 °C in a suspension containing 40% glycerol and 4% peptone, and it was routinely grown overnight in Luria-Bertani broth (LB, Sigma Aldrich) at 30 °C. For all the experiments, the cultures were diluted to an optical density of 0.4 at 600 nm.

The ATR-FTIR flow system that was used for monitoring the *E. coli* adhesion and evolution over time with and without ZA was previously reported by Delille et al. (2007). Herein, we used a ZA concentration of 1830 μM that proved to have the best ZA's anti-biofilm activity (Villa et al. 2010).

The ATR-FTIR monitors in situ and in real time the biochemical changes induced by the ZA during cell adhesion and biofilm development processes. The ATR-FTIR experiments were conducted using Jasco 610 equipped with a DTGS detector. The internal reflection element of the ATR-FTIR flow cell was a ZnSe ATR plate (50 mm × 10 mm × 6 mm), with an aperture angle of 45°, yielding 17 internal reflections. The ATR cell was sealed with a rubber O-rings. ATR-FTIR spectra acquisition was carried out between 4000 and 400 cm^{-1} as the average of 32 scans at 4 cm^{-1} resolution. The final spectra were obtained subtracting that of the corresponding cell-free broth medium from the spectra of the cell suspension. Peak fitting for the quantitative comparison was performed using PeakFit software (version 4.11, Systat). Cell adhesion on the ATR plate was monitored at the ATR-FTIR spectra at different times: 10, 20, 30, 40, 60, 90, 120, 150,180, 210, 240, and 270 min after inoculum. After the adhesion phase in a static condition, a dynamic condition with a flow rate of 0.8 mL/min was applied to remove the unbound cells from the crystal surface and promote biofilm formation. The spectra were collected at 30 min and 16 h after the initiation of the flow rate. Time-dependent changes in the spectral data were assessed by comparing the changes in the peak areas corresponding to protein and polysaccharide infrared signal between the control and the ZA-treated samples.

The cell adhesion and the biofilm development on the ATR crystal were analyzed by monitoring the variation of the characteristic absorbance profiles of the bacterial functional groups in the 1800–900 cm^{-1} spectral range. The ATR infrared spectra of *E coli* biofilm formation (Fig. 1) showed features similar to those of previously published by several authors (Quilès et al. 2016; Pousti et al. 2018; Soler-Arango et al. 2019; Stenclova et al. 2019). The most prevalent signals in these spectra originated from chemical functionalities as carboxylate, amide, phosphate, and hydroxyl groups of polysaccharides. In fact, the spectra displayed the absorption bands amides I (1635 cm^{-1}) and amide II (1546 cm^{-1}) due to C=O stretching and N-H bending of the amide bond of

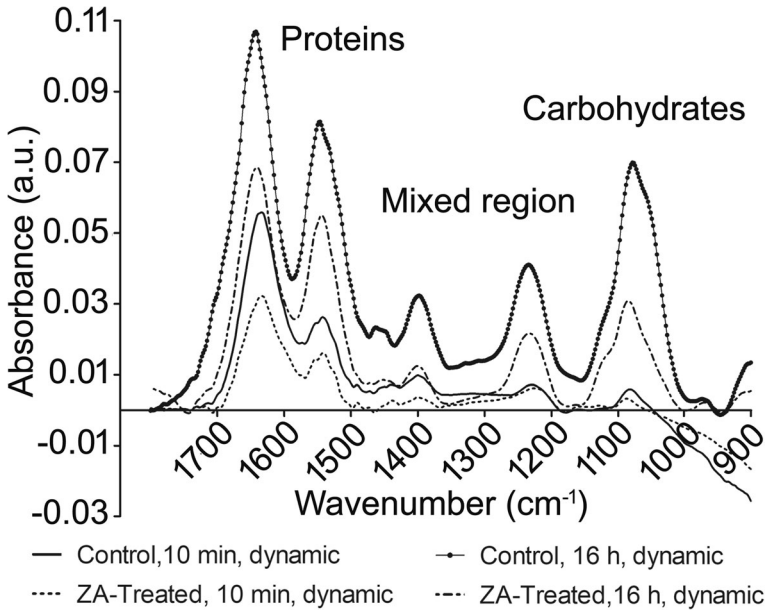

Fig. 1 Time-evolution ATR-FTIR of *E. coli* biofilms under dynamic conditions. Assignment of the IR bands are presented in Table 1

proteins, respectively. Instead, the signal in the spectral region from 1500 to 1200 cm^{-1} is due to both phospholipids and nucleic acids and that in the range 1200–900 cm^{-1} can be assigned to carbohydrates.

To estimate the difference in the biofilm growth kinetics with and without ZA, the integrated intensities of the main bands marked in Fig. 2 were calculated as a function of time. In this study, the peak area of the amide II band (1546 cm^{-1}) was used as a marker of biomass to monitor *E. coli* attachment and biofilm growth onto the ZnSe surface (Yunda et al. 2020).

Overall, during the bacterial attachment in the static phase, the intensity of the whole bacterial ATR-FTIR fingerprint with and without ZA increased over time, which reflects the bacterial colonization of the crystal (Fig. 2). During the dynamic condition, the region of the asymmetric and symmetric stretching vibrations of the phosphate groups increased, which indicates the synthesis of the nucleic acid associated with the cell division. Interestingly, during the dynamic condition, the polysaccharide band increased at a higher rate than that of the amide II, indicating the synthesis of the EPS in addition to the cell division.

The ATR-FTIR analysis confirmed that cells and the EPS macromolecules were impacted by ZA exposure, especially during the biofilm formation phase (dynamic condition). ZA exposure also modified the kinetics of biofilm development. As shown in Fig. 2a, b, *E. coli* adhesion (static condition) was strongly reduced by the 1830 μM ZA, as both the amide II and polysaccharide band areas were significantly lower than those in the control samples. Both the amide II and polysaccharides

Table 1 Assignment of the IR bands

Functional group and spectral range	Wavenumber (cm^{-1})	Vibrational modes
Proteins 1780–1480	1635 (Amide I, AmI)	>C=O stretching and C–N bending in amide group of proteins and peptides.
	1546 (Amide II, AmII)	N–H bending, C–N stretching of proteins and peptides.
Mixed region 1500–1200	1452	C-H bend in CH_2 and CH_3
	1400	>C=O symmetric stretchning of deprotonated COO^- group and C–O bending from COO^-
	1234 (nucleic acid, NA)	P=O asymmetric stretching of PO_2^- in phosphodiesters of DNA/RNA
Carbohydrates 1200–900	1169 1121 1080 (polysaccharides, PS) 1057	C–OH stretchning, C–O–C and C–O ring vibrations in polysaccharides and C–P–O stretching

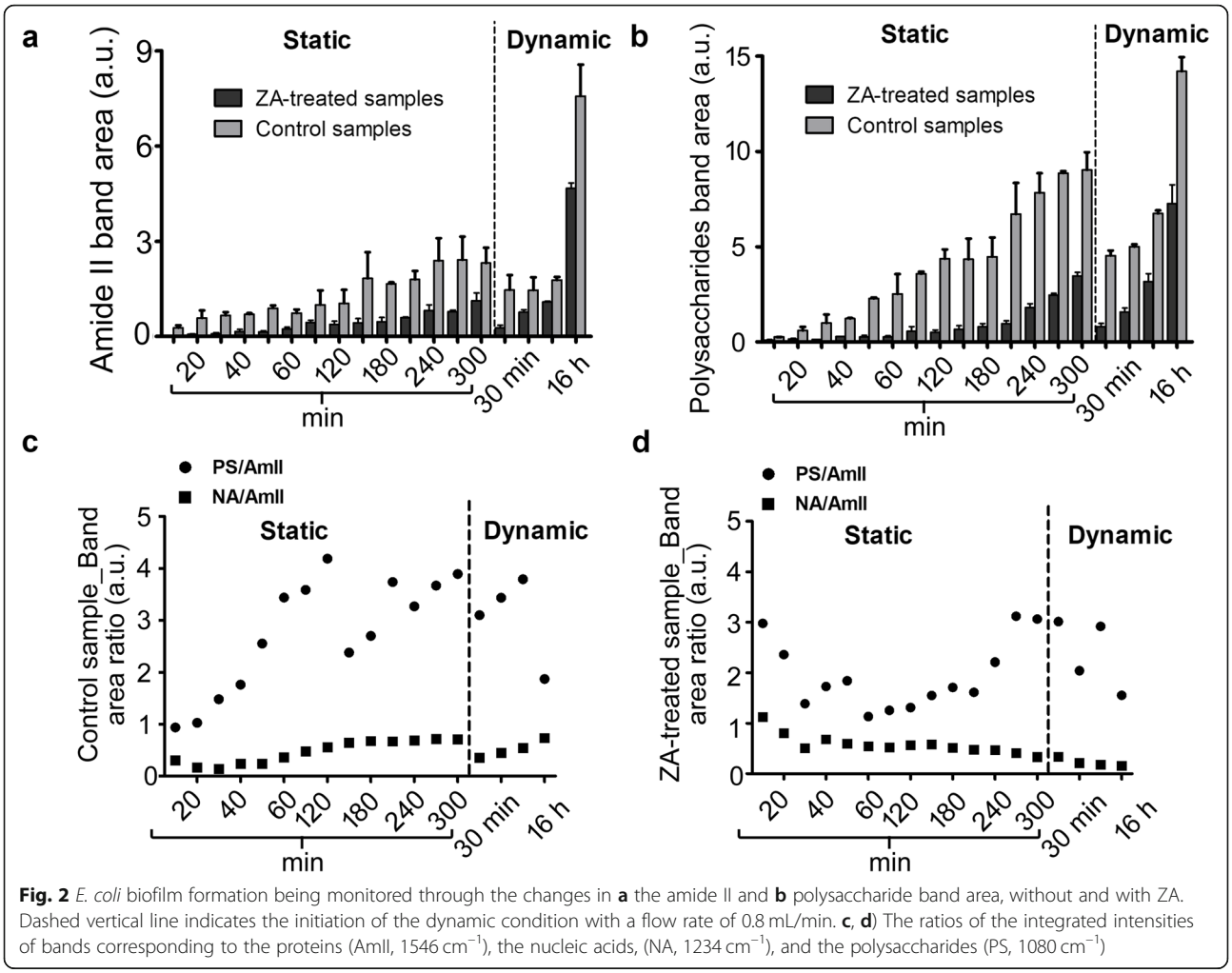

Fig. 2 *E. coli* biofilm formation being monitored through the changes in **a** the amide II and **b** polysaccharide band area, without and with ZA. Dashed vertical line indicates the initiation of the dynamic condition with a flow rate of 0.8 mL/min. **c**, **d**) The ratios of the integrated intensities of bands corresponding to the proteins (AmII, 1546 cm^{-1}), the nucleic acids, (NA, 1234 cm^{-1}), and the polysaccharides (PS, 1080 cm^{-1})

band areas became even lower under dynamic condition. The amide II (A) and the polysaccharide (PS) band areas in the untreated samples increased at higher rates than those of the treated ones ($A_{control}$: 0.384 ± 0.042 band area/h; $A_{treated}$: 0.195 ± 0.004 band area/h; $PS_{control}$: 1.515 ± 0.166 band area/h; $PS_{treated}$: 0.474 ± 0.008 band area/h). Furthermore, ZA delayed the formation of polysaccharides on the surface of the ATR plate. This finding was well described in Fig. 2c, d, in which the polysaccharide-to-amide II ratio decreased over time in the treated samples until 120 min, a trend opposite to that observed in the untreated samples. The decrease in the spectral intensity in both the proteins and polysaccharides bands of the treated samples suggested that the presence of ZA not only hindered the colonization of the ATR plate, but also weakened the cell adhesion. This finding was confirmed by the decrease of the amide II and polysaccharide band areas after the initiation of the flow in the ZA-treated samples. The nucleic acid-to-amide II ratio notably decreased over time in the treated cells, reflecting the decreasing synthesis of the nucleic acids associated with the cell division, as shown in Fig. 2d. No detectable changes in the wavenumber and the shape of the amide I and amide II bands were observed, suggesting that the ZA treatment did not induce changes in the protein's secondary structure.

All these findings—the dramatic changes in carbohydrates, proteins, and DNA profiles over time in the ZA-treated samples—are consistent with the previous results that showed the ability of ZA in hindering cell attachment and in slowing down the biofilm formation on polymeric surfaces (Dell'Orto et al. 2017; Cattò et al. 2018a, 2018b). This finding is a critical aspect in thwarting the biofilm genesis, because once the early biofilm is inhibited, the mature biofilm may in turn be prevented or at least be controlled.

The effects of the antibiofilm compound on sessile cells were investigated by observing the response of *E. coli* to ZA at the protein level, using a comparative two-dimensional gel electrophoresis approach. The biofilm developed on the ATR crystal was harvested, and total soluble cell proteins extracted as described by Suryaletha

et al. (2019). Two-hundred microgram of proteins was loaded through sample-cup loading at the cathodic end of a rehydrated strip (ImmobilineTM DryStrip gels 13 cm pH 4–7, Amersham Biosciences) and run on an Ettan ET IPGphor isoelectric focusing unit (Amersham Biosciences) for 32000 Vh. The second dimension was obtained in a vertical SDS-polyacrylamide gel using 12% (W/V) polyacrylamide resolving gel and 4% stacking gel. The separation was performed in an Ettan DALT system (Amersham Biosciences) using the following parameters: 30 min at 2 mA, 30 min at 4 mA, 30 min at 8 mA, 30 min at 16 mA, and then 3 h at 25 mA per gel. Coomassie blu-stained gels were scanned using Expression 1680 Pro scanner (Epson), and gel imaged were analyzed with Image Master^{TM}-2D (Amersham Pharmacia Biotech, little Chalfort, UK). Spots were considered to represent differentially expressed proteins if they were up or downregulated ≥ 5-fold. Protein spots to be analyzed were cut from the gels and subjected to digestion with trypsin according to standard techniques (Di Pasqua et al. 2010). The digested samples were analyzed through MALDI-TOF-MS analysis (Bruker Daltonics, Germany). Proteins showing a mascot score higher than 40 and a coverage higher than 20% were automatically validated. Identified proteins were selected among the top-scored proteins.

The whole cell proteome of *E. coli* was analyzed to study the differential protein pattern expressed by the biofilm with and without ZA. Among the 5 identified proteins, there were 2 upregulated proteins and 3 downregulated proteins in the ZA-treated samples (Fig. 3).

Overall, most of the changes in the proteomic profiles of *E. coli* biofilms occurred at the level of protein involved in stress response, DNA replication, and repair. A remarkable difference was found between the treated and the non-treated sessile cells in response to stress: the treated cells expressed higher levels of superoxide dismutase SOD than the untreated ones. In contrast, the co-chaperone GroES and the DNA repair protein RecA were downregulated in the presence of ZA.

The SODs are responsible for detoxification of toxic superoxide radicals playing an essential role in biofilm formation, resistance to oxidative stresses and bactericidal serum (Wang et al. 2018). Previous investigations suggested that ZA rendered *E. coli* planktonic cells more prone to accumulate reactive oxygen species, a stress condition to which the bacterium responded by activating defensive mechanisms against oxidative damage (Villa et al. 2011). An increase in cellular reactive oxygen species production within the biofilm might decrease the extracellular matrix and biofilm formation, as has been demonstrated for *Staphylococcus aureus* (Arce Miranda et al. 2011).

Despite the increase in oxidative stress response mechanisms, the protein folding (GroES) and DNA repair

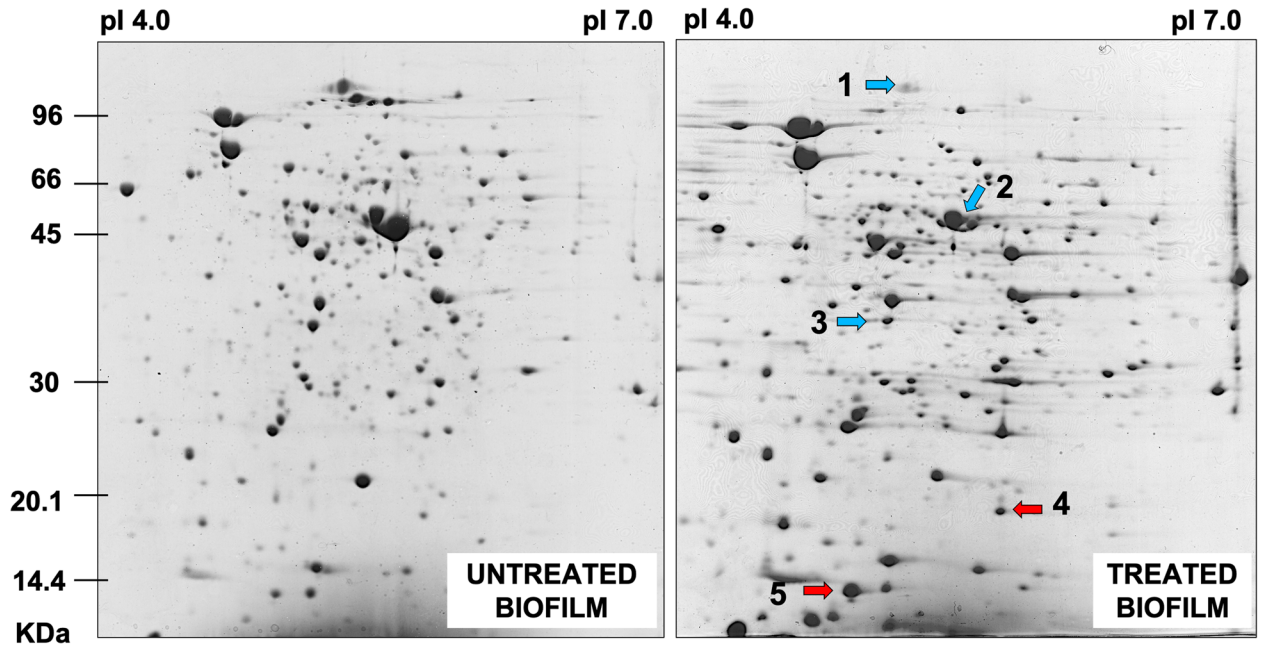

Fig. 3 Proteome expression profiles of *E. coli* biofilm-dwelling cells without (untreated biofilm) and with ZA (treated biofilm). Red arrows represent upregulated proteins; blue arrows represent downregulated proteins. Numbers in the 2D map indicate the identified proteins: (1) DNA polymerase I (*polA*), (2) elongation factor Tu 2 (*tufB*), (3) recombinase A (*recA*), (4) superoxide dismutase [Fe] (*sodB*), and (5) Chaperonin GroeS (*groS*)

(RecA) systems were downregulated by the ZA. The protein RecA also serves as the coprotease for the SOS response repressor LexA, leading to the autocatalytic cleavage of LexA that derepresses the SOS regulon and activates the DNA repair (Podlesek and Žgur Bertok 2020). Interestingly, the SOS response is strictly connected to the biofilm development. ΔRec A *Streptococcus mutans* mutants, in which the SOS response was precluded, and showed less biofilm development than the wild-type strain (Inagaki et al. 2009). In *Pseudomonas aeruginosa* experiments, the biofilm biomass was stimulated by the DNA replication inhibitor hydroxyurea at sub-inhibitory concentrations, and biofilm formation drastically diminished in *recA* knock-out mutants where the SOS was precluded (Boles et al. 2004). Since the biofilm biomass decreased when the SOS was in the off-mode, all these findings supported the inference that the SOS response contributed to the biofilm formation. This inference receives further support from a study by Costa and colleagues (Costa et al. 2014) that reported the adherence of *E. coli* K-12 strains to abiotic surfaces. The researchers concluded that the surface attachment was induced by the SOS response, since the *lexA* Ind(-) mutant did not form biofilms. Furthermore, recent findings suggested the involvement of the SOS response in the formation of *E. coli* persister cells, increasing the biofilm tolerance to the traditional antimicrobial agents (Windels et al. 2019).

The proteomic investigations revealed that the level of DNA polymerase I and the elongation factor EF-Tu protein decreased in the presence of ZA. This result was in line with the ATR-FTIR findings that indicated a decrease in the synthesis of nucleic acids associated with the cell division in the treated samples.

The EF-Tu protein is one of the most abundant cytosolic proteins that play a crucial role in protein biosynthesis (Harvey et al. 2019). The elongation factors EF-Tu has the critical function to shuttle aminoacylated tRNAs to the ribosome during the protein translation. Thus, the reduced synthesis of EF-Tu suggested that the protein synthesis capacity of *E. coli* cells was much reduced in the presence of the antibiofilm compound. The EF-Tu protein has evolved the capacity to execute the diverse functions on the extracellular surface of prokaryote cells. EF-Tu can traffic to, and is retained on, cell surfaces where it can interact with the membrane receptors and with the extracellular matrix on the surface of the plant and the animal cells (Widjaja et al. 2017; Harvey et al. 2019).

The present research showed that ZA reduced the binding capability of *E. coli* cells to ZnSe crystal, hindered firm adhesion and subsequent biofilm development on a mineral surface. The antifouling compound strongly delayed the biofilm formation and promoted the biofilm detachment. The results from this study brought forth shreds of evidence that the biofilm exposure to ZA generated significant chenges in the carbohydrates, proteins, and DNA profiles over time. This situation was translated into the reduction of the biomass and EPS contents—these effects were evident even at a brief period of ZA exposure.

In the *E. coli* sessile cells, the comparative proteome analysis revealed that while stress response was upregulated, the pathways belonging to the DNA replication and repair were downregulated in the treated biofilms. The variation of the protein patterns indicated that the presence of ZA acted as a stress factor on the sessile cells, which seems to discourage the biomass proliferation, reducing the colonization of the surface.

Overall, the results of this study provided an insight that advances current understanding of the effects of non-lethal concentration of antibiofilm compounds on bacterial biofilms growing on mineral surfaces, revealing the major pathways associated with the biofilm phenotype.

Acknowledgements
The authors acknowledge Dr. William Remelli for his contribution in 2-D Page analysis.

Authors'contributions
FV and FC designed the study and wrote the manuscript. FS performed the the ATR-FTIR analysis. FF carried out the proteomic investigation. CC helped in analysing the data. All the authors have read and approved the final version of the manuscript.

Funding
Not applicable.

Availability of data and materials
The datasets supporting the conclusions of this article are included within the article.

Ethics approval and consent to participate
This article does not contain any studies with human participants or animals performed by any of the authors.

Consent for publication
Not applicable.

Competing interests
On behalf of all authors, the corresponding author states that there is no conflict of interest.

Author details
[1]Dipartimento di Scienze per gli Alimenti, la Nutrizione e l'Ambiente, Universita` degli Studi di Milano, via Celoria 2, 20133 Milan, Italy. [2]Istituto di Scienze e Tecnologie Chimiche "Giulio Natta", Consiglio Nazionale delle Ricerche, via Mario Bianco 9, 20131 Milan, Italy.

Received: 16 November 2020 Accepted: 23 December 2020
Published online: 07 January 2021

References
Arce Miranda JE, Sotomayor CE, Albesa I, Paraje MG (2011) Oxidative and nitrosative stress in *Staphylococcus aureus* biofilm. FEMS Microbiol Lett 315: 23–29

Beloin C, Roux A, Ghigo JM (2008) *Escherichia coli* biofilms. Curr Top Microbiol Immunol 322:249–289

Boles BR, Thoendel M, Singh PK (2004) Self-generated diversity produces "insurance effects" in biofilm communities. Proc Natl Acad Sci U S A 101: 16630–16635
Cattò C, Dell'Orto S, Villa F, Villa S, Gelain A, Vitali A, Marzano V, Baroni S, Forlani F, Cappitelli F (2015) Unravelling the structural and molecular basis responsible for the anti-biofilm activity of ZA. PLoS One 10:e0131519
Cattò C, James G, Villa F, Villa S, Cappitelli F (2018a) Zosteric acid and salicylic acid bound to a low density polyethylene surface successfully control bacterial biofilm formation. Biofouling 34(4):440–452
Cattò C, Villa F, Cappitelli F (2018b) Recent progress in bio-inspired biofilm-resistant polymeric surfaces. Crit Rev Microbiol 44(5):633–652
Chan S, Pullerits K, Keucken A, Persson KM, Paul CJ, Rådström P (2019) Bacterial release from pipe biofilm in a full-scale drinking water distribution system. npj Biofilms Microbi 5:9
Costa SB, Campos ACC, Pereira ACM, de Mattos-Guaraldi AL, Júnior RH, Rosa ACP, Asad LMBO (2014) Adherence to abiotic surface induces SOS response in *Escherichia coli K-12* strains under aerobic and anaerobic conditions. Microbiology 160:1964–1973
Delille A, Quilès F, Humbert F (2007) In situ monitoring of the nascent *Pseudomonas fluorescens* biofilm response to variations in the dissolved organic carbon level in low-nutrient water by attenuated total reflectance-Fourier transform infrared spectroscopy. Appl Environ Microbiol 73:5782–5788
Dell'Orto S, Cattò C, Villa F, Forlani F, Vassallo E, Morra M, Cappitelli F, Villa S, Gelain A (2017) Low density polyethylene functionalized with antibiofilm compounds inhibits *Escherichia coli* cell adhesion. J Biomed Mater Res A 105(12):3251–3261
Di Pasqua R, Mamone G, Ferranti P, Ercolini D, Mauriello G (2010) Changes in the proteome of *Salmonella enterica* serovar Thompson as stress adaptation to sublethal concentrations of thymol. Proteomics 10:1040–1049
Galié S, García-Gutiérrez C, Miguélez EM, Villar CJ, Lombó F (2018) Biofilms in the food industry: health aspects and control methods. Front Microbiol 9:898
Harvey KL, Jarocki VM, Charles IG, Djordjevic SP (2019) The diverse functional roles of elongation factor Tu (EF-Tu) in microbial pathogenesis. Front Microbiol 10:2351
Inagaki S, Matsumoto-Nakano M, Fujita K, Nagayama K, Funao J, Ooshima T (2009) Effects of recombinase a deficiency on biofilm formation by *Streptococcus mutans*. Oral Microbiol Immunol 24:104–108
Li Q, Zhang B, Yang X, Ge Q (2018) Deterioration-associated microbiome of stone monuments: structure, variation and assembly. Appl Environ Microbiol 84: e02680–e02617
Podlesek Z, Žgur Bertok D (2020) The DNA damage inducible SOS response is a key player in the generation of bacterial persister cells and population wide tolerance. Front Microbiol 11:1785
Pousti M, Joly M, Roberge P, Amirdehi MA, Bégin-Drolet A, Greener J (2018) Linear scanning ATR-FTIR for chemical mapping and high-throughput studies of *Pseudomonas* sp. biofilms in microfluidic channels. Anal Chem 90(24): 14475–14483
Procópio L (2019) The role of biofilms in the corrosion of steel in marine environments. World J Microbiol Biotechnol 35(5):73
Quilès F, Saadi S, Francius G, Bacharouche J, Humbert F (2016) In situ and real time investigation of the evolution of a *Pseudomonas fluorescens* nascent biofilm in the presence of an antimicrobial peptide. Biochim Biophys Acta 1858(1):75–84
Soler-Arango J, Figoli C, Muraca G, Bosch A, Brelles-Mariño G (2019) The Pseudomonas aeruginosa biofilm matrix and cells are drastically impacted by gas discharge plasma treatment: a comprehensive model explaining plasma-mediated biofilm eradication. PLoS One 14(6):e0216817
Stenclova P, Freisinger S, Barth H, Kromka A, Mizaikoff B (2019) Cyclic changes in the amide bands within *Escherichia coli* biofilms monitored using real-time infrared attenuated Total reflection spectroscopy (IR-ATR). Appl Spectrosc 73(4):424–432
Suryaletha K, Narendrakumar L, John J, Radhakrishnan MP, George S, Thomas S (2019) Decoding the proteomic changes involved in the biofilm formation of *Enterococcus faecalis* SK460 to elucidate potential biofilm determinants. BMC Microbiol 19:146
Villa F, Albanese D, Giussani B, Stewart P, Daffonchio D, Cappitelli F (2010) Hindering biofilm formation with zosteric acid. Biofouling 26(6):739–752
Villa F, Pitts B, Stewart PS, Giussani B, Roncoroni S, Albanese D, Giordano C, Tunesi M, Cappitelli F (2011) Efficacy of zosteric acid sodium salt on the yeast biofilm model *Candida albicans*. Microb Ecol 62(3):584–598
Villa F, Remelli W, Forlani F, Vitali A, Cappitelli F (2012) Altered expression level of *Escherichia coli* proteins in response to treatment with the antifouling agent zosteric acid sodium salt. Environ Microbiol 14:1753–1761
Wang Y, Yi L, Zhang J, Sun L, Wen W, Zhang C, Wang S (2018) Functional analysis of superoxide dismutase of *Salmonella typhimurium* in serum resistance and biofilm formation. J Appl Microbiol 125(5):1526–1533
Widjaja M, Harvey KL, Hagemann L, Berry IJ, Jarocki VM, Raymond BBA, Tacchi JL, Gründel A, Steele JR, Padula MP, Charles IG, Dumke R, Djordjevic SP (2017) Elongation factor Tu is a multifunctional and processed moonlighting protein. Sci Rep 7:11227
Windels EM, Michiels JE, Fauvart M, Wenseleers T, Van den Bergh B, Michiels J (2019) Bacterial persistence promotes the evolution of antibiotic resistance by increasing survival and mutation rates. ISME J 13:1239–1251
Yunda E, Alem H, Francius G, Gago R, Quilès F (2020) Chemical functionalization of the zinc selenide surface and its impact on *Lactobacillus rhamnosus* GG biofilms. ACS Appl Mater Interfaces 12:14933–14945

Publisher's Note